

THE TIDAL TORQUE THEORY REVISITED. I. PROTOHALO ANGULAR MOMENTUM

EDUARD SALVADOR-SOLÉ AND ALBERTO MANRIQUE¹¹*Institut de Ciències del Cosmos. Universitat de Barcelona, E-08028 Barcelona, Spain*

ABSTRACT

In the tidal torque theory, the angular momentum (AM) of dark matter halos arises from the tidal torque suffered by non-spherical protohalos due to their surrounding mass fluctuations. This theory was implemented in the peak model where collapsing patches are ellipsoidal. However, the delimitation of the ellipsoids adopted was uncertain, and the protohalo mass used was doubtful. In addition, the numerical average of the AM of individual protohalos compromised the traceability of the functionality of the result. Last but not least, the halo AM was derived without taking into account shell-crossing and mergers. Here, we re-derive the protohalo AM in the peak model, using the natural delimitation of ellipsoids from the accurate protohalo masses and following a novel approach that clarifies the origin of its functionality. As a bonus, we obtain a very simple fully analytic expression of the protohalo AM. These results will be used in Paper II to infer the rotational properties of relaxed halos, accounting for those non-linear effects.

Keywords: methods: analytic — cosmology: theory, dark matter — dark matter: halos — galaxies: halos

1. INTRODUCTION

Dark matter halos are believed to acquire their angular momentum (AM) through the tidal torque of neighboring mass fluctuations on their seeds (Hoyle et al. 1949), which is known as the tidal torque theory (TTT). Peebles (1969) found that this mechanism does not work for spherical protohalos, but Doroshkevich (1970) and White (1984) showed that it does work in the case of more general shapes due to the misalignment of the protohalo inertia tensor with respect to the gravitational tidal tensor.

Specifically, in the Zel'dovich (1970) approximation holding to first order in perturbed quantities, by Taylor expanding to second order the deformation tensor around the center of mass (c.o.m.) of the protohalo and integrating over its volume, White (1984) found that the Cartesian components of the protohalo AM, \mathbf{J} , grow with time t according to

$$J_i(t) \approx -a^2(t)\dot{D}(t)\epsilon_{ijk}T_{jl}I_{lk}. \quad (1)$$

where ϵ_{ijk} is the fully antisymmetric Levi-Civita rank-three tensor, $T_{jl} = \partial^2\Phi/\partial x_j\partial x_l$ is the tidal tensor (equal to the shear tensor in the linear regime), i.e. the Hessian of the peculiar gravitational potential Φ at the protohalo c.o.m., and I_{lk} is the protohalo inertia tensor with respect to that point. The growth of J_i is thus encoded in

the factor $a^2(t)\dot{D}(t)$, where $a(t)$ and $D(t)$ are the cosmic scale and linear growth factor, respectively, the remaining factor being the so-called Lagrangian protohalo AM, independent of the arbitrary initial time t_i where it is calculated.

The AM growth of *individual* protohalos according to equation (1) was studied analytically (White 1984; Hoffman 1986; Catelan & Theuns 1996a) and numerically (Efstathiou & Jones 1979; Barnes & Efstathiou 1987). The results confirmed the validity of this equation roughly until protohalos reach turnaround and rapidly contract so that the AM basically freezes out (Peebles 1969).

To determine the *typical* AM of halos of different masses M , Heavens & Peacock (1988), Hoffman (1988), and Catelan & Theuns (1996b) (see also Ryden 1988; Quinn & Binney 1992; Eisenstein & Loeb 1995) implemented equation (1) in the peak model of structure formation, where collapsing patches correspond to (triaxial) density maxima in the Gaussian-smoothed density field and are thus ellipsoidal (Doroshkevich 1970), although with unknown extension and collapse time. In doing this, they found a typical halo AM proportional to $M^{5/3}$, as observed in simulations, although a factor ~ 3 higher (Barnes & Efstathiou 1987; Sugerman, Summers & Kamionkowski 2000; Porciani, Dekel, & Hoffman 2002a,b).

Whether this discrepancy was due to the neglect in this derivation of non-linear effects or to the uncertain protohalo extension and collapse time assumed in these

works is hard to tell. Indeed, these authors used the time of top-hat spherical collapse, and delimited the protohalo ellipsoids in an unnatural way that led to protohalo masses that do not conform with the usual mass of CDM objects. In addition, the dependence of the protohalo AM on the sharpness, shape, and shear field of peaks prevented these authors from averaging those properties of individual protohalos in a fully analytical manner, so the results were in a format (Hoffman 1988 used static Monte Carlo simulations and Heavens & Peacock 1988 and Catelan & Theuns 1996b included several concatenated numerical integrals) that did not facilitate the comprehension of the predicted typical AM properties.

However, since the publication of these works, a powerful formalism, the so-called *ConflUent System of Peak Trajectories* (CUSP), has been developed (see the recapitulation in Salvador-Solé & Manrique 2021) that provides the tools appropriate to address the problem of the origin of the halo AM. In fact, CUSP has been crucial in derive, directly from peak statistics and without free parameters, the halo density and kinematic profiles (Salvador-Solé et al. 2012a,b, 2023), substructure (Salvador-Solé, Manrique & Botella 2022a,b; Salvador-Solé et al. 2022), mass function (Juan et al. 2014b), and primary and secondary biases (Salvador-Solé & Manrique 2024; Salvador-Solé et al. 2024), all predictions being in full agreement with the results of simulations.

The aim of the present Paper and a forthcoming one (Paper II) is to revisit the TTT following a novel approach that remedies the shortcomings of previous works. Specifically, instead of dealing with the global shear field causing the torque, we split it into the contribution of individual neighboring (positive and negative) mass fluctuations. This allows us to characterize them and make physically motivated approximations enabling us to clarify the origin of the typical protohalo AM properties and obtain a simple fully analytic expression. In this strategy, CUSP plays a crucial role as it provides: i) accurate extensions and collapse times of ellipsoidal patches (Juan et al. 2014); ii) the connection between the properties of neighboring mass fluctuations and the protohalo (Manrique & Salvador-Solé 1995); and iii) the correlation between all these objects (Salvador-Solé & Manrique 2024). The results obtained will be used in Paper II to derive the rotational properties of halos, taking into account the effects of virialization and major mergers (Salvador-Solé et al. 2012a; Salvador-Solé & Manrique 2021).

The layout of the Paper is as follows. In Section 2 we recall some elements of CUSP entering the calculations. In Section 3, we explain our strategy and the plan of the work. The protohalo inertia tensor and the tidal tensor of neighboring mass fluctuations are derived in Sections 4 and 5, respectively. In Section 6 we compute the typical protohalo AM. Our results are summarized and discussed in Section 7.

2. THE CUSP FORMALISM

Next, we briefly explain some results of CUSP that will be used in our derivation. Interested readers are referred to the works cited in the following for more details.

2.1. Accurate Protohalo Extension and Collapse Time

As well known, the collapse time t_c of ellipsoidal patches at t_i depends not only on their size and mass, like in spherical collapse, but also on their concentration and shape (e.g. Peebles 1980), or equivalently, on the scale R , height ν (the density contrast δ scaled to its r.m.s. value σ_0), curvature or sharpness x (minus the Laplacian scaled to its r.m.s. value σ_2), ellipticity e , and prolateness p of the associated peaks in the Gaussian-smoothed density field. However, e and p depend only on the curvature, whose probability distribution function (PDF) is very sharply peaked (see below), so all peaks with fixed δ and R collapse essentially at the same time t_c .

Therefore, choosing the scale $R(M, t_c, t_i)$ of protohalos with fixed δ at t_i that evolve at t_c (in the cosmology under consideration) into haloes of different masses M (according to the chosen halo mass definition, i.e. their characteristic overdensity), all protohalos associated with peaks with $\delta(t_c, t_i)$ at scale $R(M, t_c, t_i)$ will collapse, by construction, at the same time, regardless of their mass M .

Juan et al. (2014) showed that the functions $M(R, t_c, t_i)$ and $t_c(\delta, t_i)$ setting the extension (or the mass at leading order) and collapse time of protohalos associated with Gaussian peaks with δ at R are fully determined by the consistency conditions that: i) the halo mass function predicted by CUSP is correctly normalized, and ii) the halo density profile predicted by CUSP corresponds to the mass used to derive it. Specifically, writing the density contrast δ and scale R of peaks at t_i as proportional to their well-known counterpart in top-hat spherical collapse, denoted by index ‘th’,

$$\delta(t_c, t_i) = r_\delta(t_c) \delta^{\text{th}}(t_c, t_i) = r_\delta(t_c) \delta_c^{\text{th}}(t_c) \frac{D(t_i)}{D(t_c)} \quad (2)$$

$$\begin{aligned} \sigma_0(R, t_c, t_i) &= r_\sigma(M, t_c) \sigma_0^{\text{th}}(M, t_i) \\ &= r_\sigma(M, t_c) \sigma_0^{\text{th}}(M, t_c) \frac{D(t_i)}{D(t_c)}, \end{aligned} \quad (3)$$

where $\delta_c^{\text{th}}(t)$ is the critical linearly extrapolated density contrast for top-hat spherical collapse at t , equal to 1.686 in the Einstein-de Sitter (EdS) cosmology, the proportionality functions $r_\delta(t_c)$ and $r_\sigma(M, t_c)$ corresponding to any given cosmology and halo mass definition are well fitted by the analytic functions given in Salvador-Solé & Manrique (2024). The previous relations imply in turn

$$\nu(M, t_c, t_i) = \frac{r_\delta(t_c)}{r_\sigma(M, t_c)} \nu^{\text{th}}(M, t_i). \quad (4)$$

Equation (3) gives implicitly the scale R as a function of M , t_c , and t_i through the 0th Gaussian and top-hat spectral moments. However, for power-law spectra $P(k, t_0) = P_0 k^{-n}$, where t_0 is the present time, R can be directly related to its top-hat counterpart R^{th} , satisfying, at leading order, $M = 4\pi/3\bar{\rho}(t_i)(R^{\text{th}})^3$, where $\bar{\rho}(t)$ is the mean cosmic density at t . Indeed, in this case, the j th spectral moments for Gaussian and top-hat filters f read

$$(\sigma_j^f)^2(R^f) = \frac{P_0 D_0 / D(t)}{2\pi^2 (R^f)^{n+3+2j}} \int_0^\infty dx x^{n+2(1+j)} (W^f)^2(x), \quad (5)$$

where $D_0 = D(t_0)$, so their ratio leads to

$$R(M, t_c, t_i) = r_R(M, t_c) R^{\text{th}}(M, t_i), \quad (6)$$

with

$$r_R(M, t_c) = [Q_0 r_\sigma(M, t_c)]^{\frac{-2}{n+3}}, \quad (7)$$

where $Q_0^2 \equiv \int_0^\infty dx x^{n+2} W^2(x) / \int_0^\infty dx x^{n+2} (W^{\text{th}})^2(x)$, being W and W^{th} the Fourier transforms of the Gaussian and top-hat filters, respectively. Since the cold dark matter (CDM) spectrum is locally of the power-law form (with $n \approx -1.75$ and $Q_0 \approx 0.6$ in the galaxy mass range), we can adopt the simpler relation (6). In the particular case of virial masses (i.e. characterized by virial overdensities with respect to the cosmic mean density; Bryan & Norman 1998), we are led to $r_R = 2$, that is, $R(M, t_c, t_i)$ is independent of t_c (and cosmology) and equal to $2R^{\text{th}}(M, t_i)$.

It may be argued that these protohalo extensions and collapse times rely on CUSP. That is true, but there is no doubt about the goodness of CUSP, as evidenced by all its successful results, listed in Section 1.

For simplicity in the notation, we skip from now on, unless necessary, the argument t_i in all quantities referring to the (arbitrary) initial time, as well as the argument R of the spectral moments σ_j .

2.2. Continuous Peak Trajectories

The functions $\delta(t_c)$ and $R(M, t_c)$ define a correspondence between halos and peaks. This correspondence is not merely statistical; it relates individual halos with M at t_c to peaks with δ at R in the density field at t_i . Indeed, the general relation

$$\frac{\partial \delta(\mathbf{r}, R)}{\partial R} = R \nabla^2 \delta(\mathbf{r}, R) \equiv -x(\mathbf{r}, R) R \sigma_2 \quad (8)$$

holding for Gaussian smoothing shows that, when the smoothing scale R is increased, the density contrast δ of individual peaks decreases, which conforms with the fact that the previous functions $\delta(t_c)$ and $R(M, t_c)$ are monotonically decreasing and increasing functions of t and M , respectively. Moreover, the relation (8) allows

one to identify peaks (essentially at the same fixed point) tracing the same halo at infinitesimally close smoothing scales R (see Manrique & Salvador-Solé (1995) for details).

Therefore, the mass growth of any individual accreting halo traces a continuous peak trajectory in the δ - R plane. Specifically, the peak trajectory associated with one accreting halo is the solution, for the suited boundary condition, of the differential equation (see eq. [8]),

$$\frac{d\delta}{dR} = -x[R, \delta(R)] R \sigma_2, \quad (9)$$

where $x[R, \delta(R)]$ is the curvature of the peak at the point $(\delta(R), R)$ of the trajectory. Individual peak trajectories are hard to calculate because they depend on the particular realization of the density field around the peak. However, they zigzag around the *mean* peak trajectory, solution of equation (9) with the curvature $x[R, \delta(R)]$ replaced by the mean curvature $\langle x \rangle[R, \delta(R)]$ and the same boundary condition. We can thus adopt such mean trajectories for the typical evolution of peaks in the δ - R plane.

The mean curvature of peaks with δ at R is (BBKS)

$$\langle x \rangle(R, \nu) = \frac{G_1(\gamma, \gamma\nu)}{G_0(\gamma, \gamma\nu)}, \quad (10)$$

where

$$G_i(\gamma, \gamma\nu) = \int_0^\infty dx x^i F(x) \frac{e^{-\frac{(x-\gamma\nu)^2}{2(1-\gamma^2)}}}{[2\pi(1-\gamma^2)]^{1/2}} \quad (11)$$

$$F(x) \equiv \frac{(x^3 - x) \left\{ \text{erf} \left[\left(\frac{5}{2} \right)^{\frac{1}{2}} x \right] + \text{erf} \left[\left(\frac{5}{2} \right)^{\frac{1}{2}} \frac{x}{2} \right] \right\}}{2 + \left(\frac{2}{5\pi} \right)^{\frac{1}{2}} \left[\left(\frac{31x^2}{4} + \frac{8}{5} \right) e^{-\frac{5x^2}{8}} + \left(\frac{x^2}{2} - \frac{8}{5} \right) e^{-\frac{5x^2}{2}} \right]},$$

$\gamma \equiv \sigma_1^2/(\sigma_0\sigma_2)$, and $x_* \equiv \gamma\nu = \gamma\delta/\sigma_0$. As shown by BBKS, $\langle x \rangle$ takes the form $\gamma\nu + \theta(\gamma, \gamma\nu)$ with the function θ negligible at large scales as corresponding to the large-scale mass fluctuations causing torques (see Sec. 5). Consequently, in the case of power-law spectra (and the CDM spectrum) for which $R^2\sigma_2 \propto \sigma_0$, the mean trajectories of such peaks satisfy (see eq. [9])

$$\frac{d \ln \delta}{d \ln R} = m, \quad (12)$$

where $m = -(n+3)/2$. For simplicity in the notation, we skip from now on, unless necessary, the arguments of the curvature moments and write $\langle x \rangle$, $\langle x^2 \rangle$, and so on.

Continuous peak trajectories are interrupted when the corresponding accreting halos merge. Thus, trajectories starting at peaks with δ_0 at R_0 will reach a maximum scale $R_{\text{max}}(\delta_0, R_0)$, equal to the typical separation between those peaks, where the corresponding accreting halos get in contact and merge.

2.3. Correlation between Peaks

At first order of the ‘perturbative bias expansion’, the correlation $\xi_p(r)$ between peaks with δ at R reads $\xi_p(r) = B_1^2(R, \nu)\xi(r)$, where $\xi(r)$ is the matter correlation function (well fitted by $(r/s_0)^{-\tilde{\gamma}}$, with $\tilde{\gamma} \approx 2$ and $s_0 \sim 15h^{-1}$ Mpc; [Abdullah et al. 2024](#)) and

$$B_1(R, \nu) = 1.6 \frac{\nu - \gamma \langle x^2 \rangle / \langle x \rangle}{\sigma_0 (1 - \gamma^2)} \quad (13)$$

is the Lagrangian linear peak bias derived by [Salvador-Solé & Manrique \(2024\)](#) using CUSP.

2.4. Peaks and Holes

The peak model was developed to deal with protohalos as local maxima in the linear Gaussian random density field at t_i . But in this Paper we will also be concerned with local minima or holes. Fortunately, the statistics of peaks is the same as of holes, except for the sign of the eigenvalues of the Laplacian of the density field at the peak. Thus, all expressions derived for peaks can be readily extended to holes by simply changing the sign of the trace x of the scaled Laplacian. (The ellipticity and prolateness of peaks and holes are also defined in terms of the Laplacian eigenvalues, though they are always defined with positive sign.)

This comment applies, in particular, to the continuous peak trajectories and the peak-peak correlation, which can be readily extended to holes. The only noticeable difference between continuous trajectories of peaks and holes is that the former trace, as mentioned, the mass growth of accreting halos, and the latter do not trace the mass evolution of voids because underdense regions do not collapse; they only deepen. In other words, continuous hole trajectories only trace the same fixed voids seen at different scales.

3. STRATEGY

The usual approach followed to calculate the typical AM of protohalos of mass M collapsing at t_c (or with δ at R) is to compute the protohalo inertia tensor \mathbf{I} , the tidal (or deformation) tensor \mathbf{T} at the protohalo c.o.m., and use the joint PDF of all quantities appearing in those tensors, $P(q_1, q_2, q_3, \dots | \delta, R)$ to average the modulus of the protohalo \mathbf{J} given by equation (1).

Instead, we will calculate the tidal tensor \mathbf{T}_{ts} due to each individual neighboring tidal source, proceed in the usual way to find the AM caused by it, \mathbf{J}_{ts} , integrate the AM due to all sources, and average the resulting global J over all possible configurations of the composite system.

The joint PDF $P(q_1, q_2, q_3, \dots | \delta, R)$ of properties q_i appearing in the torque caused by each single torque source will be split into the product of the conditional probability P_{ts} of finding the properties q_1, q_2, q_3, \dots subject to having found the protohalo with the properties $\tilde{q}_1, \tilde{q}_2, \tilde{q}_3, \dots$ times the probability P_{pk} that the protohalo of

given δ at R has such properties,

$$P(q_1, q_2, q_3, \dots | \delta, R) = P_{ts}(q_1, q_2, q_3, \dots | \tilde{q}_1, \tilde{q}_2, \tilde{q}_3, \dots) \times P_{pk}(\tilde{q}_1, \tilde{q}_2, \tilde{q}_3, \dots | \delta, R). \quad (14)$$

This facilitates concentrating, in Section 4, in the calculation of the protohalo inertia tensor and the PDF of the protohalo (or peak) properties, $P_{pk}(\tilde{q}_1, \tilde{q}_2, \tilde{q}_3, \dots | \delta, R)$, and, in Section 5, in the calculation of the tidal tensor due to one torque source and the conditional PDF of the torque source properties subject to having found the protohalo with some properties, $P_{ts}(q_1, q_2, q_3, \dots | \tilde{q}_1, \tilde{q}_2, \tilde{q}_3, \dots)$. Then, the resulting PDFs will be used in Section 6 to integrate and average the protohalo AM.

It is also worth mentioning that it will often happen that some property q_i , e.g. q_2 , or some property \tilde{q}_i , e.g. \tilde{q}_2 , does not correlate with the remaining properties. In this case, it will disappear from the respective conditional PDF, though not from the global joint PDF, where its own PDF will appear as an isolated factor, e.g.

$$P(q_1, q_3, \dots | \delta, R) = P_{ts}(q_2) P_{pk}(\tilde{q}_2) P_{ts}(q_1, q_3, \dots | \tilde{q}_1, \tilde{q}_3, \dots) \times P_{pk}(\tilde{q}_1, \tilde{q}_3, \dots | \delta, R). \quad (15)$$

4. PROTOHALO

The conditional PDF of finding in an infinitesimal volume at t_i a peak with some given curvature, shape (i.e. ellipticity and prolateness), and orientation (Euler angles α , β , and κ), $C = (x, e, p, \alpha, \beta, \kappa)$, subject to having density contrast δ (or height $\nu = \delta/\sigma_0$) at R is $P_{pk}(C | \nu, R) = \mathcal{N}_{pk}(\nu, C, R)$, where

$$\mathcal{N}_{pk}(\nu, C, R) = \frac{e^{-\frac{\nu^2}{2}}}{4\pi^2 R_\star^3} \frac{F(x) e^{-\frac{(x-\gamma\nu)^2}{2(1-\gamma^2)}}}{[2\pi(1-\gamma^2)]^{\frac{1}{2}}} P_{ep}(e, p) P_E(\alpha, \beta, \kappa), \quad (16)$$

is the average number density of peaks with those properties (BBKS). In equation (16), $R_\star \equiv \sqrt{3}\sigma_1/\sigma_2$, $P_E(\alpha, \beta, \kappa)$ is the usual isotropic PDF of Euler angles,¹ and

$$P_{ep}(e, p) \approx \frac{1}{2\pi\sigma_e\sigma_p} e^{-\frac{(e-\langle e \rangle)^2}{2\sigma_e^2} - \frac{(p-\langle p \rangle)^2}{2\sigma_p^2}} \quad (17)$$

is the joint PDF of ellipticities $e = (\lambda_1 - 2\lambda_2 + \lambda_3)/(2x)$ ($e \geq 0$) and prolatenesses $p = (\lambda_1 - \lambda_3)/(2x)$ ($-e \leq p \leq e$), where $\lambda_1 \geq \lambda_2 \geq \lambda_3$ are minus the eigenvalues of the Laplacian, related to the peak curvature through $\lambda_1 + \lambda_2 + \lambda_3 = x$. To write equation (17), we have taken

¹ The orientation of triaxial peaks does not depend on their remaining properties, so the set of properties C in the conditional probability $P_{pk}(C | \nu, R)$ is reduced to $C = (x, e, p)$.

into account that, for large x as for the massive halos of interest, $P_{\text{ep}}(e, p)$ is nearly Gaussian with means $\langle e \rangle = 1/\{\sqrt{5x}[1+6/(5x^2)]^{1/2}\}$ and $\langle p \rangle = 6/\{5x^4[1+6/(5x^2)]^2\}$ and dispersions $\sigma_e = \langle e \rangle/\sqrt{6}$ and $\sigma_p = \langle e \rangle/\sqrt{3}$ (BBKS). This reflects the fact that, as mentioned, the peak shape correlates with the height ν only through x .

As mentioned, the second factor on the right of equation (16) giving the x -PDF is very sharply peaked, so the average of any function $f(x)$ is essentially equal to $f(\langle x \rangle)$. This allows us to marginalize the curvature and work with x replaced by $\langle x \rangle(R, \delta)$ everywhere.² This leads to

$$P_{\text{pk}}(C|\nu, R) = P_{\text{ep}}(e, p)\mathcal{N}_{\text{pk}}(\nu, R), \quad (18)$$

with $C = (e, p)$ and

$$\mathcal{N}_{\text{pk}}(\nu, R) = \frac{G_0(\gamma, \gamma\nu)}{(2\pi)^2 R_\star^3} e^{-\frac{\nu^2}{2}} \quad (19)$$

giving the average number density of peaks with ν at R .

The inertia tensor \mathbf{I} of the ellipsoidal protohalo relative to its c.o.m. in Cartesian coordinates oriented along the principal axes is

$$\mathbf{I} = \frac{M}{5a^2(t_i)} \begin{pmatrix} \iota_1 & 0 & 0 \\ 0 & \iota_2 & 0 \\ 0 & 0 & \iota_3 \end{pmatrix}, \quad (20)$$

where $\iota_1 \equiv a_2^2 + a_3^2$, $\iota_2 \equiv a_1^2 + a_3^2$ and $\iota_3 \equiv a_2^2 + a_1^2$, being $a_1 > a_2 > a_3$ the semi-axes of the ellipsoidal protohalo at t_i . To write equation (20) we have taken into account that equation (1) holds to first order in perturbed quantities and the tidal tensor is necessarily of first order because caused by *peculiar* mass fluctuations, so we can take the density of the protohalo to leading order, i.e. with uniform density equal to $\bar{\rho}(t_i)$. Thus, \mathbf{I} is a Lagrangian tensor (it does not depend on t) independent of t_i , as expected.

The semi-axes a_i of the (non-smoothed) protohalo are completely fixed by its (accurate) extension R (or R^{th}). Indeed, the mass $M = 4\pi/3\bar{\rho}(t_i)a_1a_2a_3$ of the ellipsoid is, by definition of R^{th} , equal $4\pi/3\bar{\rho}(t_i)(R^{\text{th}})^3$, which implies

$$a_i = R^{\text{th}} \left(\frac{\Lambda}{\lambda_i} \right)^{1/2}, \quad (21)$$

where $\Lambda \equiv (\lambda_1\lambda_2\lambda_3)^{1/3}$. Thus, defining the scaled semi-axes as

$$\hat{a}_i \equiv \frac{a_i}{R^{\text{th}}} \left(\frac{x}{\Lambda} \right)^{1/2} \quad (22)$$

² The e - and p -PDFs are less peaked, so it is preferable not to make a similar approximation for these quantities.

(with x replaced by $\langle x \rangle$), the relations given above between the peak shape and eigenvalues, we obtain

$$e = \frac{1}{2}(1 - \hat{a}_2^{-2}) \quad \text{and} \quad p = \frac{1}{2}(\hat{a}_1^{-2} - \hat{a}_3^{-2}). \quad (23)$$

We stress that the protohalo ellipsoid has been delimited in the usual way: from their mass M and their uniform density (to linear order in perturbed quantities) $\bar{\rho}(t_i)$, by simply taking into account their shape. In spherical objects, this leads to their top-hat radius R^{th} through the relation $M = 4\pi/3\bar{\rho}(t_i)(R^{\text{th}})^3$. Similarly, in ellipsoid objects with known ellipticity and prolateness (those of the associated peaks), the relation $M = 4\pi/3\bar{\rho}(t_i)a_1a_2a_3$ leads to the top-hat semi-axes. Note also that the inertia tensor is $\propto (R^{\text{th}})^5 \propto M^{5/3}$ simply because the semi-axes a_i are $\propto R^{\text{th}}$.

5. TORQUE SOURCES

The torque suffered by a protohalo is caused by neighboring *positive and negative* mass fluctuations, marked by density maxima (peaks) with positive height, and density minima (holes) with negative height, respectively. For the moment, we will concentrate in the torque caused by mass excesses, and postpone the case of mass defaults to the end of the Section.

Mass excesses of scale smaller than the scale R of the protohalo do not contribute to the tidal torque. Their individual effect is weak and they are very numerous and roughly isotropically distributed around the protohalo, so their added effect cancels (particularly when averaging over all configurations; Sec. 6). On the other hand, many of the large-scale mass excesses actually correspond to a few real ones responsible for the torque, seen at different scales. We must thus find those ‘authentic’ mass excesses, hereafter denoted by index ‘a’.³

Each series of embedded large-scale mass excesses trace a continuous peak trajectory, solution of equation (12), i.e. of the form $\delta'(R') = \delta'(R)(R'/R)^m$, starting at some peak, hereafter called the ‘reference peak’, with the minimum scale R and a density contrast $\delta'(R)$ different in general from the density contrast δ of the protohalo (but see below). Given that m is negative ($m \approx -0.63$ for CDM in the relevant mass range), $\delta'(R')$ decreases with increasing R' , though less rapidly than $(R')^{-3}$, so the mass excess $\delta(R')(R')^3$ increases with increasing scale. Therefore, the scale R_a of the authentic mass excess is limited by the typical maximum scale $R_{\text{max}}(R, \delta'(R))$ of those peak trajectories (see Sec. 2.2) and the separation r between their c.o.m. and the c.o.m. of the protohalo (ellipsoidal shells, or homoeoids, exceeding r do not contribute to the gravitational potential at the c.o.m. of the protohalo; see below).⁴ Thus, au-

³ Dubbing them as ‘effective’ would be more appropriate, but index ‘e’ is already occupied by ellipticities.

⁴ The protohalo itself is embedded in a similar mass excess, so $r > R_a$.

thentic mass excesses have $R_a = \min\{R_{\max}[R, \delta'(R)], r\}$ and $\delta_a = \delta'(R)(R_a/R)^m$.

The conditional probability that an authentic mass excess of scale R_a with ν_a and $C_a = (e_a, p_a, \alpha_a, \beta_a, \kappa_a)$ lies at a distance r from the c.o.m. of the protohalo is

$$P_a(\nu_a, C_a, R_a, r|\delta, C, R) = 4\pi r^2 \int_{-\infty}^{\infty} d\delta' [1 + \xi_{\text{pk}}(r; \nu_a, R_a, \nu, R)] \times \mathcal{N}_{\text{pk}}(\nu_a, C_a, R_a|\delta', R) P(\delta', R, r|\delta, C, R), \quad (24)$$

where $P(\delta', R, r|\delta, C, R)$ is the probability of finding a point with δ' at a distance r from the peak with δ and C in the density field smoothed at scale R , $\mathcal{N}_{\text{pk}}(\nu_a, C_a, R_a|\delta', R)$ is the average conditional number density of peaks with ν_a and C_a at R_a subject to have δ' at R , and $1 + \xi_{\text{pk}}(r; \nu_a, R_a, \nu, R)$ is the factor enhancing this number density due to the cross-correlation between peaks with δ at R and with δ_a at R_a .⁵

Both $\mathcal{N}_{\text{pk}}(\nu_a, C_a, R_a|\delta', R)$ and $P(\delta', R, r|\delta, C, R)$ were calculated by BBKS. But we do not need the explicit form of the former. As shown in Appendix A, for massive halos, as corresponding to bright galaxies, and separations r not too large compared to R , as corresponding to the protohalo neighborhood, $P(\delta', R, r|\delta, C, R)$ turns out to be null for all values of δ' except for $\delta' \approx \delta$. In other words, it is close to a Dirac delta independent of C . This remarkable result is a consequence of the well-known protohalo bias, i.e. the more massive objects are, the more clustered, together with the rapid fall of the (proto)halo mass function with increasing mass. Both effects imply that close pairs of protohalos of the same scale tend to be twin, i.e. to have the same density contrast (though not necessarily the same shape and orientation). Thus, equation (24) becomes

$$P_a(\nu_a, C_a, R_a, r|\delta, C, R) \approx 4\pi r^2 [1 + \xi_{\text{pk}}(r; \nu_a, R_a, \nu, R)] \mathcal{N}_{\text{pk}}(\nu_a, C_a, R_a|\delta, R) = 4\pi r^2 [1 + \xi_{\text{pk}}(r; \nu, R)] \mathcal{N}_{\text{pk}}(\nu, C_a, R) \equiv P_a(C_a, r|\delta, R). \quad (25)$$

To write the first equality on the right of equation (25), we have taken into account that δ_a and R_a are functions of δ and R of the reference peak, through the relations $R_a = \min[R_{\max}(\delta, R), r]$ and $\delta_a = \delta'(R)(R_a/R)^m$, with $\delta'(R) = \delta$. And in the second equality, we have taken into account that the probability of finding the peak with ν_a at R_a is the same as of finding the reference peak with ν at R at the same point, so the cross-correlation ξ_{pk} between the protohalo and authentic mass excess equals the autocorrelation between identical peaks. Thus, the conditional probability P_a be-

comes

$$P_a(C_a, r|\delta, R) = 4\pi r^2 [1 + B_1^2(R, \nu)\xi(r)] \mathcal{N}_{\text{pk}}(\nu, C_a, R) \quad (26)$$

in terms of the linear peak bias B_1 (Sec. 2).

Like all patches marked by peaks, authentic mass excesses are ellipsoidal with semi-axes a_{a1} , a_{a2} , and a_{a3} .⁶ In addition, to first order in perturbed quantities, they have a uniform ‘peculiar density’ equal to $\delta(t_i)\bar{\rho}(t_i)$. Consequently, the peculiar gravitational potential they cause, in Cartesian coordinates with origin at their c.o.m. and aligned with their own principal axes, at a point $\mathbf{x} = (x_1, x_2, x_3)$ external to it is (e.g. Chandrasekhar 1987)

$$\Phi_a(\mathbf{x}) = \pi a_{a1} a_{a2} a_{a3} G \delta_a \bar{\rho}(t_i) \times \left[\int_{S(\mathbf{x})}^{\infty} \frac{ds}{\Delta(s)} - \sum_{i=1}^3 x_i^2 \int_{S(\mathbf{x})}^{\infty} \frac{ds}{(a_{ai}^2 + s)\Delta(s)} \right] \quad (27)$$

(the potential of homoeoids at internal points vanishes), where G is the gravitational constant, $M_a = 4\pi/3 a_{a1} a_{a2} a_{a3} \delta_a(t_i) \bar{\rho}(t_i)$ is the peculiar mass,

$$\Delta(s) \equiv [(a_{a1}^2 + s)(a_{a2}^2 + s)(a_{a3}^2 + s)]^{1/2}, \quad (28)$$

and $S(\mathbf{x})$ denotes the positive root of equation

$$\sum_{i=1}^3 \frac{x_i^2}{a_{ai}^2 + S} = 1. \quad (29)$$

Thus, taking the Hessian of this potential, we obtain the tidal tensor at the point \mathbf{x} equal to c.o.m. of the protohalo (see App. B)

$$T_{aij} \approx \frac{a^3(t_i)}{D(t_i)} \frac{4\pi}{3} G \delta_a \bar{\rho}(t_i) \left(\frac{R_a^{\text{th}}}{r} \right)^3 \left[3 \frac{x_i x_j}{a_{ai}^2 a_{aj}^2} - \delta_{ij} \right]. \quad (30)$$

As can be seen this tensor, which is also Lagrangian (it does not depend on t) and independent of t_i , is proportional to δ_a .

Let us come back now to mass defaults also contributing to the torque. For the reasons explained in Section 2.4, the preceding derivation for mass excesses (and peaks) also holds for mass defaults (and holes), with the only difference that, in the latter case, δ_a and $\langle x_a \rangle$ are negative. Since the number density contrast of peaks with positive δ at R is $\delta_{\text{pk}} = B_1(R, |\nu|)\delta_m$ and that of holes with negative δ at R is $\delta_h = -B_1(R, |\nu|)\delta_m$ (see eq. 13), the peak-hole cross-correlation is given by

⁵ The point with δ' at R essentially coincides with the reference peak of the authentic mass excess.

⁶ This is certainly true for high peaks (BBKS); for low ones it is an approximation. But we are only interested in the peculiar gravitational potential they yield, which is much less sensitive to small departures of the sources from the ellipsoidal symmetry.

$\xi_{\text{pkh}}(r) = -B_1^2(R, |\nu|)\xi(r)$. Consequently, the probability of finding an authentic large-scale mass excess *or* default, from now on, simply, a torque source, with δ_a at R_a at a distance r from the protohalo is $P_a(C_a|\delta, R, r)$ given by equation (26) but a factor two higher and no bias term arising from the correlation between sources because the peak-peak correlation exactly cancels with the peak-hole one, i.e.

$$P_a(C_a, r|\delta, R) = 8\pi r^2 \mathcal{N}_{\text{pk}}(\nu, C_a, R). \quad (31)$$

The fact that the protohalo-torque source correlation vanishes when both peaks and holes are taken into account is well-understood: given a peak, the probability of finding other peaks in its neighborhood is higher than in the average, but the probability of finding holes is lower, and both effects balance each other. This result has important consequences in the calculations next.

6. PROTOHALO ANGULAR MOMENTUM

Given a protohalo of mass M and collapse time t_c (or with δ and R), the components, in a Cartesian reference system with origin at its c.o.m., of its Lagrangian AM with respect to that point due to the torque of one source only is (eq. [1])

$$J_{ai} = -\epsilon_{ijk} [R_a T_a R_a^T]_{jl} [R I R^T]_{lk}, \quad (32)$$

where \mathbf{I} and \mathbf{T}_a are the Lagrangian inertia tensor of the protohalo and the Lagrangian tidal tensor due to that torque source, both oriented along their own axes, given in Sections 4 and 5, respectively, and \mathbf{R} and \mathbf{R}_a , with index T denoting transpose, the rotation (or direction cosine) matrices in order to reorient them along the Cartesian reference axes. Therefore, to find the *typical* AM of protohalos we must sum up the contribution to the AM due to every single torque source in a given configuration and average the result over all possible configurations (mutual separations, shapes, and orientations of all objects). This task may seem unfeasible, but, as shown next, the absence of correlation between the protohalo and the torque sources and between torque sources themselves makes it possible.

The torque strength of individual sources behaves as $(R_a)^3 \delta_a / r^3$, with bounded $R_a = \min[R_{\text{max}}(R, \delta), r]$, so, for fixed δ_a , the strength decreases with increasing r or stays at most constant for torque sources at small r . But, since $\delta_a = (R_a/R)^m \delta$ decreases with increasing $R_a = \min[R_{\text{max}}(R, \delta), r]$, the strongest torque source is necessarily the closest one to the protohalo. Since the closest torque necessarily lies at a separation r from the protohalo smaller than or equal to the mean separation between peaks with δ at R , its R_a is equal to r . This result will be used to simplify the form of the tidal tensor (eq. [30]), and, what is more important here, it greatly simplifies the integration of the contribution of all sources in one configuration of the system and the average over all configurations.

Given that the N -point correlations vanish,⁷ all objects are uncorrelated. Therefore, they are randomly distributed around any particular subsystem, such as the one formed by the protohalo and the nearest torque source, so, when averaging over all configurations with fixed protohalo-nearest torque source subsystem, the added torque of all the remaining sources cancel. We may thus concentrate in averaging over all possible configurations of the protohalo-nearest torque source only.

The probability of finding the *nearest* torque source with C_a at a distance r from the protohalo is the probability of finding one such torque source inside r times the probability that there is none at smaller separations (see eq. [31]),

$$P_{\text{st}}(C_a, r|\delta, R) = 8\pi r^2 \mathcal{N}_{\text{pk}}(\nu, C_a, R) \times \left[1 - \frac{8\pi}{3} r^3 \mathcal{N}_{\text{pk}}(\nu, C_a, R) \right]. \quad (33)$$

Therefore, the joint PDF of the protohalo-nearest torque source properties to be used in the average of J_a given by equation (32) (though referring to the nearest torque source) over all configurations of this subsystem is $P_E(\alpha, \beta, \kappa, \alpha_a, \beta_a, \kappa_a) P_E(\alpha, \beta, \kappa)$ times

$$P_{\text{st}}(C_a, C, r|\delta, R) = P_{\text{st}}(C_a, r|\delta, R) P_{\text{pk}}(C|\delta, R), \quad (34)$$

with $C_a = (e_a, p_a)$, $C = (e, p)$, and the conditional probabilities P_{pk} and P_{st} given by equations (18) and (33), respectively.

We will start by averaging J_a over the uncorrelated orientations of the protohalo and the nearest torque source, i.e. over the Euler angles α, β, κ and $\alpha_a, \beta_a, \kappa_a$. Of course, we must not average the components J_{ai} themselves, but the modulus of \mathbf{J}_a . However, by isotropy of the universe, the averaged absolute magnitude of any component $|J_{ai}|$ must be the same, implying $\langle J_a \rangle^2 = 3 \langle |J_{ai}|^2 \rangle$. Consequently, the average modulus can be calculated from the average absolute magnitude of any given component. The result is (App. C)

$$J_a = \sqrt{3} J_{ai} \approx \frac{G \bar{\rho}_0^{1/3} M^{5/3}}{20 \times 3^{1/2}} \left(\frac{R_a}{r} \right)^3 \left(\frac{R_a}{R} \right)^m \frac{\delta}{D(t_i)} \times H(e_a, p_a) \left(\frac{1 - 2e}{1 + e} \right)^{2/3} p, \quad (35)$$

where $\bar{\rho}_0 = \bar{\rho}(t_0)$, and $H(e_a, p_a)$ is a function of the ellipticity and prolateness of the torque source, given in equation (C15). We remark that the factor $\delta = \delta(t_c, t_i)$ arises from the peculiar density of torque sources, written in terms the density contrast of the protohalo, and

⁷ The extension of the two-point to $N > 2$ involves the reduced N -point correlations, which, in case of peaks, write approximately down as $N - 1$ products of two-point correlations (e.g. Suto & Matsubara 1994).

the factor $M^{5/3}$ arises from the inertia tensor, multiplied by an extra factor $\bar{\rho}^{2/3}(t_i)$ coming from the tidal torque sources (the remaining $\bar{\rho}^{1/3}(t_i)$ gives rise to the factor $\bar{\rho}_0^{1/3}$).

By then averaging over the ellipticity and prolateness of the protohalo and of the nearest torque source, we arrive at (App. D)

$$J_a \approx 0.0434 G \bar{\rho}_0^{1/3} g(\gamma, \gamma\nu) M^{5/3} \left(\frac{R^{\text{th}}}{r} \right)^{-\frac{5m}{3}} \left(\frac{r_R}{2} \right)^2 \frac{\delta}{D(t_i)}, \quad (36)$$

where

$$g(\gamma, \gamma\nu) \equiv \left[\frac{(\gamma\nu)^{1/3}}{\langle x \rangle^2 + 6/5} \right]^2. \quad (37)$$

To obtain equation (36) we have neglected $|(3p)/(1+e)|$ in front of unity (not only is $|p| \leq e$, but, for peaks of galactic mass, $|p| \ll 1$) and $|(2e_a - 1)/3| \lesssim 0.3$ in front of negative powers of the same quantity.

Lastly, averaging over all possible separations r of the nearest torque source for $P_{\text{st}}(r|\delta, R)$ given by equation (34), with no C_a and C arguments since already averaged, i.e.

$$P_{\text{st}}(r|\delta, R) = 8\pi r^2 \mathcal{N}_{\text{pk}}(\nu, R) \left[1 - \frac{8\pi}{3} r^3 \mathcal{N}_{\text{pk}}(\nu, R) \right], \quad (38)$$

over all possible separations of the nearest torque source. That is, we must perform the integral

$$J = \int_0^{r_{\text{one}}(\delta, R)} dr J_a(r, \delta, R) P_{\text{st}}(r|\delta, R), \quad (39)$$

where

$$r_{\text{one}} = R \left[\frac{2}{3\pi} \left(\frac{n+5}{6} \right)^{3/2} G_0(\gamma, \gamma\nu) e^{-\frac{\nu^2}{2}} \right]^{-\frac{1}{3}} \quad (40)$$

is the radius of the sphere centered at the c.o.m. of the protohalo that harbors one torque source, solution of the implicit equation

$$1 = 8\pi R^3 \mathcal{N}_{\text{pk}}(\nu, R) \int_0^{\frac{r_{\text{one}}}{R}} ds s^2, \quad (41)$$

with $\mathcal{N}_{\text{pk}}(\nu, R)$ given by equation (19). Note that r_{one}/R is independent of t (ν is time-invariant) and of t_i .

At this point, it is worth mentioning that, following the previous derivation for protohalos conditioned to lie in a background δ_m at scale $R_m > 3R$ instead of unconditioned ones, we would be led to equation (41) with the torque source number density \mathcal{N}_{pk} including an additional term proportional to $\nu\delta_m/\sigma_0$ for peaks, and another for holes (see Salvador-Solé et al. 2024). But since

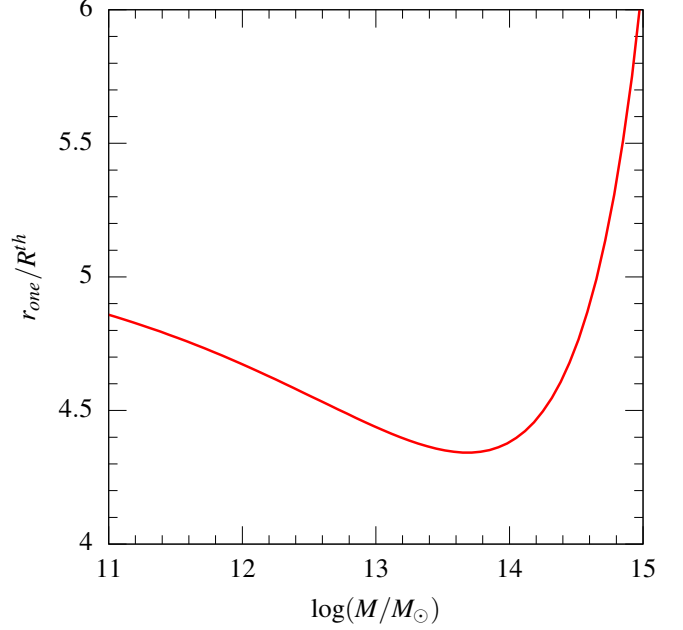


Figure 1. Typical time-invariant maximum separation (about twice the median value) between the centers of mass of the protobhalo and the mass fluctuation responsible of the main tidal torque, in units of the typical protohalo (top-hat) radius, as a function of halo virial mass in the *Planck14* (Planck Collaboration et al. 2014) cosmology.

ν has the opposite sign in peaks and holes, those additional terms would cancel and $r_{\text{one}}/R^{\text{th}}$ would remain the same. The reason for this is simple: in overdense backgrounds there are more peaks, but also less holes, and conversely in underdense backgrounds. The result that r_{one} does not vary with background density was used in Salvador-Solé et al. (2024) in the study of the secondary bias of halo AM.

In Figure 1 we plot $r_{\text{one}}/R^{\text{th}}$ in the *Planck14* (Planck Collaboration et al. 2014) cosmology and for virial masses ($R^{\text{th}} = R/2$). Even though $r_{\text{one}}/R^{\text{th}}$ depends on M , it is kept quite constant (~ 4.5) except at the very high-mass end, where the halo number density falls off and their typical separation rapidly increases.

With this value of r_{one} , the final average (39) leads to the desired mean Lagrangian protohalo AM,

$$J \approx \frac{0.150}{5m/3+3} G \bar{\rho}_0^{1/3} g(\gamma, \gamma\nu) M^{5/3} \left(\frac{R^{\text{th}}}{r_{\text{one}}} \right)^{-\frac{5m}{3}} \left(\frac{r_R}{2} \right)^2 \frac{\delta}{D(t_i)} \quad (42)$$

to leading order in $R^{\text{th}}/r_{\text{one}}$ (next term is $O[(R^{\text{th}}/r_{\text{one}})^3]$ smaller). Note that J does not depend on t_i because r_R is a function of M and t_c only (eq. [7]) and δ stands for $\delta(t_c, t_i) = r_\delta(t_c)D(t_i)/D(t_c)$ (eq. [2]). This Lagrangian AM is plotted in Figure 2. As can be seen, J is essentially proportional to $M^{5/3}$, as found in simulations

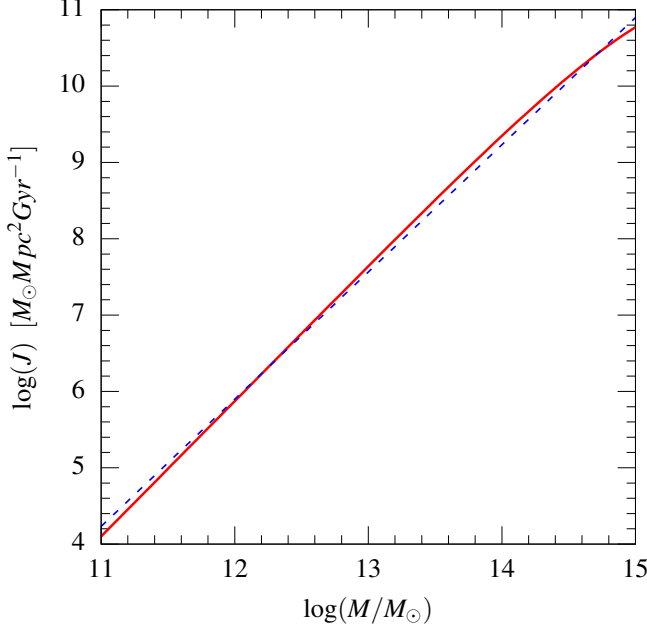


Figure 2. Mean Lagrangian protohalo AM (solid red line) as a function of mass in the *Planck14* cosmology and for virial masses. The straight dashed blue line shows the best fit to a simple $M^{5/3}$ law.

(e.g. Barnes & Efstathiou 1987; Sugerman, Summers & Kamionkowski 2000).

To end up, using the previous joint PDF, we can also calculate the median protohalo AM, J_{med} . The Euler angles have flat PDFs and do not enter J_{med} . The uncorrelated PDFs of the ellipticities and prolatenesses of the protohalo and the nearest torque source are Gaussian, so their median values are equal to their well-known means. Lastly, the median separation, r_{med} , is given by the value of r for which the cumulative PDF ($\approx 8\pi r^2 \mathcal{N}_{\text{pk}}(\nu, \delta)$; eq. [38]) is one half, i.e. the solution of the implicit equation

$$0.5 \approx \frac{\int_0^{r_{\text{med}}} dr r^2}{\int_0^{r_{\text{one}}} dr r^2} = \left(\frac{r_{\text{med}}}{r_{\text{one}}} \right)^3, \quad (43)$$

which leads to $r_{\text{med}} \approx 0.5^{1/3} r_{\text{one}}$. Plugging all these median values in the non-averaged protohalo AM (eq. [35] with $R_a = r$ as corresponding to the nearest torque source) and using the relation $\langle x_a \rangle \approx (r/R)^m \gamma \nu$ (see App. D), we are led to

$$J_{\text{med}} \approx \frac{0.79(5m/3 + 3)}{2^{11m/9}} \tilde{g}(\gamma, \gamma \nu) J \quad (44)$$

where

$$\tilde{g}(\gamma, \gamma \nu) \approx \left(1 + \frac{\langle x \rangle}{27} \right) \left[1 - \frac{3}{(5\langle x \rangle^2 + 6)^{-1/2} + 1} \right]^{2/3}. \quad (45)$$

Taking into account that $-5m/3 \approx 1.05$, that $\langle x \rangle$ is of order unity for halos of bright galaxies, and that r_δ in

equation (2) is very approximately unity in all cosmologies, the mean and median Lagrangian protohalo AM adopt the approximate compact form

$$J \approx 0.015 G \bar{\rho}_0^{-1/3} g(\gamma, \gamma \nu) M^{5/3} \left(\frac{r_R}{2} \right)^2 \frac{\delta}{D(t_i)} \approx J_{\text{med}}. \quad (46)$$

7. SUMMARY AND DISCUSSION

We have derived the typical Lagrangian protohalo AM predicted by the TTT within the peak model of structure formation. This has been done following a novel approach that splits the global tidal tensor into the contributions of individual neighboring mass fluctuations. The interest of this procedure is that it allows one to average the AM of protohalos of mass M collapsing at t_c in a fully analytic manner, which is crucial to clarify the origin of its properties.

After characterizing the positive and negative mass fluctuations of all scales contributing to the global torque and taking into account their correlation, we have integrated the AM they cause and averaged over all configurations. After a few justified approximations we have obtained the following fully analytic expression of the mean Lagrangian AM, essentially equal to the median value J_{med} ,

$$J \approx 0.015 G \bar{\rho}_0^{-1/3} g(\gamma, \gamma \nu) M^{5/3} \left[\frac{r_R(M, t_c)}{2} \right]^2 \frac{r_\delta(t_c) \delta_c^{\text{th}}(t_c)}{D(t_c)}, \quad (47)$$

where $\bar{\rho}_0$ is the present mean cosmic density, $g(\gamma, \gamma \nu)$ is a very weak functions of M given by equation (37), $\delta_c^{\text{th}}(t) \approx 1.686$ is the critical density contrast for top-hat spherical collapse at t , $D(t)$ is the cosmic growth factor, and $r_R(M, t_c)$ and $r_\delta(t_c)$ are two functions provided by CUSP (see e.g. Salvador-Solé & Manrique 2024) setting the accurate extension and ellipsoidal collapse time of protohalos associated with Gaussian peaks. The factor $r_R(M, t_c)$ depends on halo mass definition, but it is always close to two, the exact value for virial masses. Similarly, r_δ depends on cosmology, but it is always close to unity, the exact value for the EdS cosmology. Equation (47) stands for the CDM spectrum approximated to a power-law of index $n = -1.75$ suited to the range of bright galaxy halos, but the expression for power-law spectra of any index n is also given.

The most important result compared to previous similar works (Heavens & Peacock 1988; Hoffman 1988; Catelan & Theuns 1996b) is that, thanks to the accurate (mass definition-dependent) $M(R)$ provided by CUSP, it has been possible to delimit protohalos in the usual natural way: from their mass M , their shape (provided in this case by the ellipticity and prolateness of their associated peaks), and their density to leading order equal to $\bar{\rho}(t_i)$. This has led to protohalo semi-axes, $a_i \propto R^{\text{th}}$, masses, $M \propto (R^{\text{th}})^3$, and AM, $J \propto (R^{\text{th}})^5$, satisfying the relation $J \propto M^{5/3}$.

In the absence of an accurate mass $M(R)$ of protohalos with Gaussian scale R at t_i , ellipsoids were delimited in previous works by choosing a threshold isodensity contour around peaks. This led to semi-axes $a_i \propto \nu^{1/2}$, masses $M \propto \nu^{3/2}$, and AM $J \propto \nu^{5/2}$. However, since the relation between the Gaussian and top-hat heights, ν and ν^{th} , was unknown, the relation $M \propto \nu^{3/2}$ could not be compared with the relation $M \propto (\nu^{\text{th}})^{6/(n+3)}$ of CDM objects. In fact, the proportionality factor in that relation included the quantity R_* , whose value, dependent on the spectral index n , was considered independent of ν , so M and ν were independent variables. However, the height ν of peaks with R cannot be dissociated from n . As shown here, when the accurate mass of protohalos with scale R is taken into account, ν is found to be proportional to ν^{th} (for the appropriate n fixing R_*), and the relation $M \propto \nu^{3/2}$ is equivalent to a relation $M \propto (\nu^{\text{th}})^{3/2}$ different from $M \propto (\nu^{\text{th}})^{6/(n+3)}$. This means that the protohalo delimitation used in those works was wrong, and, consequently, led to a deficient AM estimate.

Despite this, [Heavens & Peacock \(1988\)](#), [Hoffman \(1988\)](#), and [Catelan & Theuns \(1996b\)](#) also found the relation $J \propto M^{5/3}$. This relation was found after averaging the AM of protohalos with various powers of the mass at fixed ν . But, as shown here, this relation is more fundamental than this: *it arises directly from the protohalo inertia tensor of individual protohalos*. In fact, this was already implicit in the expressions of the mass and AM of individual protohalos found in those works (see e.g. eqs. [21]-[22] in [Catelan & Theuns 1996b](#)).

This intrinsic origin of the relation $J \propto M^{5/3}$ implies, in turn, that the common belief that it is due to the halo bias is wrong. This belief was based on the idea that the more massive (proto)halos, the larger their AM because they are more clustered and suffer stronger torques. However, this is not the case. The clustering of halo is responsible for the AM bias due to the dependence of the protohalo AM on $\langle x \rangle$ through the factor $g(\gamma, \gamma\nu)$ (see [Salvador-Solé et al. 2024](#) for details), but it does not cause the $J \propto M^{5/3}$ relation. Even though peaks are correlated, holes are anticorrelated by the same strength with respect to protohalos, so the average torque due to neighboring positive *and* negative mass fluctuations is the same everywhere, both

in high density regions where positive mass fluctuations are predominant and in low density regions where negative mass fluctuations are.

[Heavens & Peacock \(1988\)](#), [Hoffman \(1988\)](#), and [Catelan & Theuns \(1996b\)](#) used their predicted Lagrangian protohalo AM to estimate the typical halo AM. However, in the absence of an accurate ellipsoidal collapse time $t_c(\delta)$ of protohalos with density contrast δ at t_i , they took the spherical collapse time t_c^{th} . In the EdS cosmology, where $D(t) = a(t)$ so that the Eulerian protohalo AM, equal to the Lagrangian AM multiplied by $\dot{D}(t)a^2(t)$, grows as t , neglecting non-linear effects, they found that the final halo AM was typically a factor $t_c^{\text{th}}/t_i \propto [D(t_c^{\text{th}})/D(t_i)]^{3/2} \propto (\delta^{\text{th}})^{-3/2}$ (or $\propto (\nu^{\text{th}})^{-3/2}$) larger than at t_i . However, was it for the deficient Lagrangian protohalo AM or for the spherical collapse time used (or both), the estimate of the halo AM appeared to be a factor ~ 3 larger than found in simulations. Having derived here the right Lagrangian protohalo AM, we could readily integrate the corresponding Eulerian AM up to the right (cosmology-dependent) ellipsoidal collapse time provided by CUSP to find a new estimate of the halo AM. However, this estimate would not yet account for non-linear effects. Since CUSP also provides the clues for properly accounting for shell-crossing and halo mergers ([Salvador-Solé et al. 2012a](#); [Salvador-Solé & Manrique 2021](#)), we prefer to postpone the whole calculation to Paper II, where we will characterize, in addition, the spin and all inner rotational properties of dark matter halos.

ACKNOWLEDGMENTS

This work was funded by the Spanish MCIN/AEI/10.13039/501100011033 through grants CEX2019-000918-M (Unidad de Excelencia ‘María de Maeztu’, ICCUB) and PID2022-140871NB-C22 (co-funded by FEDER funds) and by the Catalan DEC through the grant 2021SGR00679.

DATA AVAILABILITY

The data underlying this article will be shared on reasonable request to the corresponding author.

REFERENCES

- Abdullah, M. H., Klypin, A., Prada, F., Wilson, G., Ishiyama, T., Ereza, J. 2024, MNRAS, 529, L545
- Bardeen, J. M., Bond, J. R., Kaiser, N., Szalay, A. S., 1986 ApJ, 304, 15 (BBKS)
- Barnes, J., Efstathiou, G. 1987, ApJ, 319, 575
- Bryan, G. L., & Norman, M. L. 1998, ApJ, 495, 80
- Catelan, P. & Theuns, T. 1996a, MNRAS, 282, 436
- Catelan, P. & Theuns, T. 1996b, MNRAS, 282, 455
- Chandrasekhar, S. 1987, efe..book
- Doroshkevich, A. G. 1970, Astrophysics, 6, 320
- Efstathiou, G. & Jones, B. J. T. 1979, MNRAS, 186, 133
- Eisenstein, D. J. & Loeb, A. 1995, ApJ, 439, 520.
doi:10.1086/175193
- Henry, J. P. 2000, ApJ, 534, 565

- Hoffman, Y. 1986, *ApJ*, 301, 65
- Hoffman, Y. 1988, *ApJ*, 329, 8
- Hoyle, F., Burgers, J. M., van de Hulst, H. C. 1949, eds., in *Problems of Cosmical Aerodynamics*, Central Air Documents Office, Dayton, p. 195
- Juan, E., Salvador-Solé, E., Domènec, G., Manrique, A. 2014, *MNRAS*, 439, 719
- Juan, E., Salvador-Solé, E., Domènec, G., Manrique, A. 2014b, *MNRAS*, 439, 3156
- Komatsu, E., Smith, K. M., Dunkley, J., Bennett, C. L., Gold, B., Hinshaw, G., Jarosik, N., et al. 2011, *ApJS*, 192, 18L137
- Manrique, A. & Salvador-Solé E. 1995, *ApJ*, 453, 6
- Manrique, A. & Salvador-Solé E. 1996, *ApJ*, 467, 504
- Heavens, A. & Peacock, J. 1988, *MNRAS*, 232, 339
- Peebles, P. J. E. 1969, *ApJ*, 155, 393
- Peebles, P. J. E. 1980, *Large-Scale Structure of the Universe* by Phillip James Edwin Peebles. Princeton University Press, 1980. ISBN: 978-0-691-08240-0
- Planck Collaboration, Ade, P. A. R., Aghanim, N., et al. 2014, *A&A*, 571, AA16
- Porciani, C., Dekel, A., Hoffman, Y. 2002a, *MNRAS*, 332, 325
- Porciani, C., Dekel, A., Hoffman, Y. 2002, *MNRAS*, 332, 339
- Quinn, T. & Binney, J. 1992, *MNRAS*, 255, 729
- Raig, A., González-Casado, G., & Salvador-Solé, E. 2001, *MNRAS*, 327, 939
- Ryden, B. S. 1988, *ApJ*, 329, 589. doi:10.1086/166406
- Salvador-Solé, E., Manrique, A., Solanes, J. M. 2005, *MNRAS*, 358, 901
- Salvador-Solé, E., Viñas, J., Manrique, A., & Serra, S. 2012a, *MNRAS*, 423, 2190
- Salvador-Solé, E., Serra, S., Manrique, A., & González-Casado, G. 2012b, *MNRAS*, 424, 3129
- Salvador-Solé, E., Manrique, A. 2021, *ApJ*, 914, 141
- Salvador-Solé, E., Manrique, A., Botella, I. 2022a, *MNRAS*, 509, 5305
- Salvador-Solé, E., Manrique, A., Botella, I. 2022b, *MNRAS*, 509, 5316
- Salvador-Solé, E., Manrique, A., Canales, D., Botella, I. 2022, *MNRAS*, 511, 641
- Salvador-Solé, E., Manrique, A., Canales, D., et al. 2023, *MNRAS*, 521, 1988
- Salvador-Solé, E. & Manrique, A. 2024, *ApJ*, 974, 226
- Salvador-Solé, E., Manrique, A., & Agulló, E. 2024, *ApJ*, 976, 47
- Sugerman, B., Summers, F. J., Kamionkowski, M. 2000, *MNRAS*, 311, 762
- Suto, Y. & Matsubara, T. 1994, *ApJ*, 420, 504
- White, S. D. M. 1984, *ApJ*, 286, 38
- Zel'dovich, Y. B. 1970, *A&A*, 5, 84

APPENDIX

A. PROBABILITY OF FINDING A DENSITY CONTRAST NEAR TO A PROTOHALO

The probability of finding a point with δ' at a distance r from a peak with δ and C in the density field Gaussian-smoothed on the scale R of the peak is a Gaussian with mean (BBKS)

$$\langle \delta(r) | C \rangle = \frac{\gamma\delta}{1-\gamma^2} \left(\frac{\psi}{\gamma} + \frac{\nabla^2\psi}{3} \right) - \frac{\langle x \rangle \sigma_0}{1-\gamma^2} \left(\gamma\psi + \frac{\nabla^2\psi}{3} \right) + \frac{5}{2} \langle x \rangle \sigma_0 \left(\frac{\psi'}{r} - \frac{\nabla^2\psi}{3} \right) P_{\text{ep}}(e, p) \quad (\text{A1})$$

(the curvature variance is unity) and variance

$$\langle [\Delta\delta(r)]^2 | C \rangle = \sigma_0^2 \left\{ 1 - \frac{1}{1-\gamma^2} \left[\psi^2 + \left(2\gamma\psi + \frac{\nabla^2\psi}{3} \right) \frac{\nabla^2\psi}{3} \right] - 5 \left(\frac{\psi'}{r} - \frac{\nabla^2\psi}{3} \right)^2 - \frac{3(\psi')^2}{\gamma^2} + \frac{1}{(1-\gamma^2)^2} \left(\gamma\psi + \frac{\nabla^2\psi}{3} \right)^2 \right\}, \quad (\text{A2})$$

where ψ is the matter correlation function $\xi(r)$ at scale R normalized to $\xi(0)$ and ψ' is its r -derivative, being r in units of R_* . As discussed in BBKS, for high peaks (massive halos), $\langle x \rangle$ approaches $\gamma\nu$, and the gradients of ψ can be neglected in front of unity and of ψ , which is of order unity when r is small (of order R). Consequently, $\langle [\Delta\delta(r)]^2 | C \rangle$ approaches $\hat{\sigma}_0 \equiv \sigma_0^2[1 - \psi^2] \approx 0$ and $\langle \delta(r) | C \rangle$ essentially becomes $\delta\psi \approx \delta$.

Therefore, the conditional probability $P(\delta', R, r | \delta, C, R)$ in equation (24) approaches

$$P(\delta', R, r | \delta, C, R) \approx \left[\frac{e^{-\frac{(\delta' - \delta)^2}{2\hat{\sigma}_0^2}}}{\sqrt{2\pi\hat{\sigma}_0}} \right]_{\hat{\sigma}_0 \approx 0} \approx \delta_D(\delta' - \delta), \quad (\text{A3})$$

where $\delta_D(\delta' - \delta)$ is the Dirac delta. Note that the properties C and the separation r do not appear now in P because they do not correlate with other properties, so $P(\delta', R, r | \delta, C, R)$ becomes $P(\delta', R | \delta, R)$.

B. TIDAL TENSOR

The Hessian of the Lagrangian gravitational potential (27) at a point \mathbf{x} from the torque source causing it is

$$T_{a_{ij}} \equiv \frac{a^3(t_i)}{D(t_i)} 4\pi G \delta_a(t_c, t_i) \bar{\rho}(t_i) \frac{\Delta(0)}{\Delta[S(\mathbf{x})]} \left(\frac{x_i x_j}{[a_{ai}^2 + S(\mathbf{x})][a_{aj}^2 + S(\mathbf{x})]} \left\{ \sum_{k=1}^3 \frac{x_k^2}{[a_{ak}^2 + S(\mathbf{x})]^2} \right\}^{-1} - \delta_{ij} \int_{S(\mathbf{x})}^{\infty} \frac{\Delta[S(\mathbf{x})] ds}{\Delta(s)(a_{ai}^2 + s)} \right), \quad (\text{B4})$$

where δ_{ij} is the Kronecker delta, $\Delta[S(\mathbf{x})]$ is given by equation (28) but with s replaced by $S(\mathbf{x})$ defined in equation (29).

The relation $a_{a1}a_{a2}a_{a3} = (R_a^{\text{th}})^3$ implies that the semi-axes of the putative ellipsoidal isodensity contours at \mathbf{x} with modulus r are r/R_a^{th} times the real semi-axes of the torque source. This implies in turn that $\sum_{k=1}^3 x_k^2/a_{ak}^2 = (r/R_a^{\text{th}})^2$ and $\Delta(0) = (R_a^{\text{th}})^3$. On the other hand, taking into account that the ellipticity and prolateness of peaks is moderate (BBKS) so that $S/a_{ai}^2 \approx S/(R_a^{\text{th}})^2$, we have $S(\mathbf{x}) \approx r^2 - (R_a^{\text{th}})^2$, $\Delta[S(\mathbf{x})] = r^3$, and $\Delta(0) = (R_a^{\text{th}})^3$. Consequently, the tidal tensor at the c.o.m. of the protohalo takes the form

$$T_{a_{ij}} \approx \frac{a^3(t_i)}{D(t_i)} 4\pi G \delta_a(t_c, t_i) \bar{\rho}(t_i) \left(\frac{R_a^{\text{th}}}{r} \right)^3 \left[\frac{x_i x_j}{a_{ai}^2 a_{aj}^2} - \delta_{ij} U(a_{ak}^2) \right], \quad (\text{B5})$$

In equation (B5),

$$U(a_{ak}^2) \equiv \frac{1}{2} \int_0^\infty \frac{ds/a_{aj}^2}{1 + s/a_{aj}^2} \left[\prod_{k=1}^3 \left(1 + \frac{s}{a_{ak}^2} \right) \right]^{-1/2} = \frac{1}{2} \int_1^\infty \frac{dy}{y^{3/2}} \left[\sum_{k=1}^3 \frac{a_{aj}^2 + s(y)}{a_{ak}^2 + s(y)} \right]^{-1}, \quad (\text{B6})$$

which, given that the ellipticity and prolateness of large-scale peaks is moderate (BBKS), becomes

$$U(a_{ak}^2) \approx \frac{1}{6} \int_1^\infty \frac{dy}{y^{3/2}} = \frac{1}{3}. \quad (\text{B7})$$

C. AVERAGE OVER ORIENTATIONS

Since for any spatial configuration of the protohalo-torque source subsystem there is another one yielding an AM with the same modulus and opposite sign, the average of $|J_{ai}|$ must be carried out over half the whole composite solid angle $(8\pi^2)^2$ sd.

Since the averages over the two sets of Euler angles may be carried out independently, we can start by averaging over α , β and κ in the whole solid angle $8\pi^2$ sr. The scaled inertia tensor (eq. [20]) then becomes

$$\langle I \rangle_{\alpha, \beta, \kappa} = \frac{M}{15a^2(t_i)} \begin{pmatrix} \iota_1 & 0 & 0 \\ 0 & \iota_2 & 0 \\ 0 & 0 & \iota_3 \end{pmatrix}, \quad (\text{C8})$$

and the component i of the AM reads

$$\langle J_{ai}^L \rangle_{\alpha, \beta, \kappa} = -\frac{M}{15a^2(t_i)} \epsilon_{ijk} [R_a T_a R_a^T]_{jk} \iota_k = -\frac{M}{15a^2(t_i)} [R_a T_a R_a^T]_{jk} (\iota_j - \iota_k), \quad (\text{C9})$$

with i , j , and k in the usual ciclic order.

As mentioned, the principal axes of \mathbf{I} may not coincide with those of \mathbf{T}_a . Thus, regardless of the orientation of \mathbf{T}_a , we may assume $\iota_j - \iota_k \equiv a_k^2 - a_j^2$ in equation (C9) equal to $a_3^2 - a_1^2$. This is very convenient because then we simply have (see eqs. [23]-[22])

$$a_3^2 - a_1^2 = \frac{1}{a_3^{-2}} - \frac{1}{a_1^{-2}} = \frac{a_1^{-2} - a_3^{-2}}{a_3^{-2} a_1^{-2}} = \frac{\hat{a}_1^{-2} - \hat{a}_3^{-2}}{\hat{a}_3^{-2} \hat{a}_1^{-2}} = 2p \left[\frac{(1-2e)^2}{(1+e)^2 - 9p^2} \right]^{1/3} \approx 2 \left(\frac{1-2e}{1+e} \right)^{2/3} p, \quad (\text{C10})$$

where we have neglected $|3p/(1+e)|$ in front of unity (not only is $|p| \leq e$, but, for peaks of galactic mass, we also have $|p| \ll 1$).

Consequently, we are led to

$$\langle J_{ai}^L \rangle_{\alpha, \beta, \kappa} \approx 2 \frac{M(R^{\text{th}})^2}{15a^2(t_i)} [R_a T_a R_a^T]_{jk} \left(\frac{1-2e}{1+e} \right)^{2/3} p \quad (\text{C11})$$

in terms of the ellipticity and prolateness of the peak associated with the protohalo.

We must now average over the Euler angles α_a , β_a and κ_a in $8\pi^2/2$ sr from any arbitrary initial orientation of the position vector \mathbf{r}_a of the c.o.m. of the protohalo (e.g. in the a_{ai} direction). After a lengthy calculation, we arrive at the following average of $[R_a T_a R_a^T]_{23}$, with \mathbf{T}_a given by equation (30),

$$\langle [R_a T_a R_a^T]_{23} \rangle_{\alpha_a, \beta_a, \kappa_a} = \frac{a^3(t_i) G \bar{\rho}(t_i) \delta}{24D(t_i)} \left(\frac{R_a}{r} \right)^3 \left(\frac{R_a}{R} \right)^m H(a_{ai}) \quad (\text{C12})$$

$$H(a_{ai}) \equiv \frac{4\pi-9}{36} + (R_a^{\text{th}})^2 \frac{\langle x_a \rangle}{\Lambda_a} \left\{ \frac{5\pi-8}{30} \hat{a}_{d1}^{-4} + \left(\frac{8}{9\pi} + \frac{26+75\pi}{120} \right) \hat{a}_{d1}^{-2} \hat{a}_{d2}^{-2} - \frac{1}{10} \hat{a}_{d2}^{-4} - \frac{1}{5} \hat{a}_{d1}^{-2} \hat{a}_{d3}^{-3} - \left(\frac{1}{5\pi} + \frac{3\pi}{16} \right) \hat{a}_{d2}^{-2} \hat{a}_{d3}^{-2} + \frac{4}{5} \hat{a}_{d3}^{-4} \right\}, \quad (\text{C13})$$

where we have taken into account $\delta_a = (R_a/R)^m \delta$. Taking into account the equality $\hat{a}_{ai}^{-2} = \lambda_{ai}/[\langle x_a \rangle R_a^{\text{th}}]$, $H(a_{ai})$ adopts the following approximate form as a function of e_a (or $\tilde{e}_a \equiv -(1-2e_a)/3$) and p_a

$$H(e_a, p_a) \approx \frac{1}{10} \left(1 + \frac{p_a^{-\frac{2}{3}}}{3} \left(\tilde{e}_a^{\frac{2}{3}} + \tilde{e}_a^{\frac{8}{3}} - \tilde{e}_a^{\frac{14}{3}} \right) \left\{ 1 + \frac{0.6 p_a \tilde{e}_a^{-1}}{1 + \tilde{e}_a} \left[90 - \left(\frac{1}{\tilde{e}_a} - 2 \right)^3 \right] \right\} \right) \approx \frac{1}{10} \left[1 + \frac{p_a^{-\frac{2}{3}}}{3} \left(\tilde{e}_a^{\frac{2}{3}} + \tilde{e}_a^{8/3} - \tilde{e}_a^{\frac{14}{3}} \right) \left(1 + \frac{54 p_a \tilde{e}_a^{-1}}{1 + \tilde{e}_a} \right) \right]. \quad (\text{C14})$$

Taking into account that $|\tilde{e}_a| \lesssim 0.3$, $H(e_a, p_a)$ can be further approximated to

$$H(e_a, p_a) \approx \frac{1}{10} \left\{ 1 + (\tilde{e}_a p_a)^{-1/3} \left[16 + \frac{1}{3 p_a^{4/3}} (\tilde{e}_a p_a) \right] \right\} = \frac{1}{10} \left\{ 1 - 3^{1/3} [(1-2e_a) p_a]^{-1/3} \left[16 - 3^{-2} (1-2e_a) p_a^{-1/3} \right] \right\}.$$

(C15)

Having performed those two averages, the typical value of e.g. the first Cartesian component of the Lagrangian prothalo AM takes the form

$$J_{a1} \equiv \langle \langle J_{a1} \rangle_{\alpha, \beta, \kappa} \rangle_{\alpha_a, \beta_a, \kappa_a} \approx \frac{1}{12} \frac{G \bar{\rho}_0^{1/3} \delta M^{5/3}}{5D(t_i)} \left(\frac{R_a}{r} \right)^3 \left(\frac{R_a}{R} \right)^m H(e_a, p_a) \left(\frac{1-2e}{1+e} \right)^{2/3} p, \quad (C16)$$

implying an average modulus of the Lagrangian AM equal to

$$J_a = \sqrt{3} J_{ai} \approx \frac{1}{20 \times 3^{1/2} D(t_i)} G \bar{\rho}_0^{1/3} \delta M^{5/3} \left(\frac{R_a}{r} \right)^3 \left(\frac{R_a}{R} \right)^m H(e_a, p_a) \left(\frac{1-2e}{1+e} \right)^{2/3} p. \quad (C17)$$

D. AVERAGE OVER ELLIPTICITIES AND PROLATENESSES

We must now average J_a given by equation (C17) over the ellipticity and prolateness of the prothalo and torque source. Taking into account the following averages of powers of p_a from $-e_a$ to e_a holding for massive halos, with $e_a \lesssim 0.3$ and $p_a \ll \sigma_{ap}$,

$$\langle p_a^{-1/3} \rangle(e_a) \approx \frac{6e_a^{2/3}}{\sqrt{2\pi}\sigma_{ap}} \exp \left[-\frac{\langle p_a \rangle^2}{2\sigma_{ap}^2} \right] \left[\frac{e_a \langle p_a \rangle}{5\sigma_{ap}^2} + O(e_a^3) \right] \approx \frac{6e_a^{5/3} \langle p_a \rangle}{5\sqrt{2\pi}\sigma_{ap}^3} \quad (D18)$$

$$\langle p_a^{-2/3} \rangle(e_a) \approx \frac{6e_a^{1/3}}{\sqrt{2\pi}\sigma_{ap}} \exp \left[-\frac{\langle p_a \rangle^2}{2\sigma_{ap}^2} \right] \left[1 - \frac{e_a^2 (\langle p_a \rangle^2 - \sigma_{ap}^2)}{14\sigma_{ap}^2} + O(e_a^3) \right] \approx \frac{6e_a^{1/3}}{\sqrt{2\pi}\sigma_{ap}} \left[1 + \frac{e_a^2}{14} \right], \quad (D19)$$

the averages of J_a over p and p_a lead to

$$J_a \approx \frac{2}{40\sqrt{3}} \frac{G \bar{\rho}_0^{1/3} \delta M^{5/3}}{D(t_i)} \left(\frac{R_a}{r} \right)^3 \left(\frac{R_a}{R} \right)^m H(e_a) \left(\frac{1-2e}{1+e} \right)^{2/3} \langle p \rangle, \quad (D20)$$

with

$$H(e_a) \approx \frac{1}{10} \left[1 - \frac{24 \times 3^{4/3}}{5\sqrt{2\pi}\sigma_{ap}^3} (1-2e_a)^{-1/3} e_a^{5/3} \langle p_a \rangle + \frac{2 \times 3^{-2/3}}{\sqrt{2\pi}\sigma_{ap}} (1-2e_a)^{-2/3} e_a^{1/3} \left(1 + \frac{e_a^2}{14} \right) \right], \quad (D21)$$

where $\langle p \rangle$ and $\langle p_a \rangle$ are much smaller than unity, e and e_a are also smaller than unity, and so are σ_{ap} , σ_{ae} , and $\langle e_a \rangle$, too. Thus, to leading order in such small quantities, we have

$$J_a \approx \frac{1}{200\sqrt{3}} \frac{G \bar{\rho}_0^{1/3} \delta M^{5/3}}{D(t_i)} \left(1 + \frac{2 \times 3^{-2/3}}{\sqrt{2\pi}\sigma_{gp}} e_a^{1/3} \right) \left(\frac{R_a}{r} \right)^3 \left(\frac{R_a}{R} \right)^m \langle p \rangle, \quad (D22)$$

where we have kept the term $e_a^{1/3}/\sigma_{ap}$ because it is of $O(\langle e_a \rangle^{-2/3})$. And, taking into account the following approximate average from $-(\langle e_a \rangle + 3\sigma_{ae})$ to $\langle e_a \rangle + 3\sigma_{ae} = 1.40\langle e_a \rangle$ (even though e_a is positive, it is convenient to extend the integral to negative e_a values to find the right normalization constant of the approximately normal PDF)

$$\langle e_a^{1/3} \rangle = \frac{6}{\sqrt{2\pi}\sigma_{ae}} (1.4\langle e_a \rangle)^{4/3} e^{-\frac{\langle e_a \rangle^2}{2\sigma_{ae}^2}} \left[\frac{1.4\langle e_a \rangle}{7} \frac{\langle e_a \rangle}{\sigma_{de}^2} + O(\langle e_a \rangle^3) \right] \approx \frac{6 \times 1.4^{7/3}}{7\sqrt{2\pi}} \frac{\langle e_a \rangle^{10/3}}{\sigma_{de}^3}, \quad (D23)$$

and the equalities $\sigma_{de} = \langle e_a \rangle/\sqrt{6}$ and $\sigma_{ap} = \langle e_a \rangle/\sqrt{3}$, we find, to leading order, the following average over e_a

$$J_a \approx 0.021 \frac{G \bar{\rho}_0^{1/3} \delta M^{5/3}}{D(t_i)} \left(\frac{R_a}{r} \right)^3 \left(\frac{R_a}{R} \right)^m \langle e_a \rangle^{-2/3} \langle p \rangle = 0.634 \frac{G \bar{\rho}_0^{1/3} \delta M^{5/3}}{D(t_i)} \left(\frac{R_a}{r} \right)^3 \left(\frac{R_a}{R} \right)^m \langle e_a^{-2/3} \rangle e^4. \quad (D24)$$

Lastly, expressing $\langle e \rangle$ and $\langle e_a \rangle$ as functions of $\langle x \rangle$ and $\langle x_a \rangle$ (see the comment on eq. [17]) and, taking into account that for large masses, as it is the case particularly for torque sources, the average curvature is $\langle x_a \rangle \approx \gamma \nu_a = (R_a/R)^m \gamma \nu = (\min[R_{\max}(R, \delta), r]/R)^m \gamma \nu$, where $\min[R_{\max}(R, \delta), r]/R$ is substantially larger than unity, we obtain

$$J_a \approx 0.0434 G \bar{\rho}_0^{1/3} M^{5/3} \left(\frac{r R R_a^{\text{th}}}{r} \right)^3 \left(\frac{r R R_a^{\text{th}}}{R} \right)^{5m/3} \left[\frac{(\gamma \nu)^{1/3}}{\langle x \rangle^2 + \frac{6}{5}} \right]^2 \frac{\delta}{D(t_i)}, \quad (D25)$$

Thus, the AM due to the nearest torque source is given by equation (D25) with $R_a^{\text{th}} = r/2$.